The Nonchromatin Substructures of the Nucleus: The Ribonucleoprotein (RNP)–containing and RNP-depleted Matrices Analyzed by Sequential Fractionation and Resinless Section Electron Microscopy

Edward George Fey, Gabriela Krochmalnic, and Sheldon Penman

Department of Biology, Massachusetts Institute of Technology, Cambridge, Massachusetts 02139

Abstract. The nonchromatin structure or matrix of the nucleus has been studied using an improved fractionation in concert with resinless section electron microscopy. The resinless sections show the nucleus of the intact cell to be filled with a dense network or lattice composed of soluble proteins and chromatin in addition to the structural nuclear constituents. In the first fractionation step, soluble proteins are removed by extraction with Triton X-100, and the dense nuclear lattice largely disappears. Chromatin and nonchromatin nuclear fibers are now sharply imaged.

Nuclear constituents are further separated into three well-defined, distinct protein fractions. Chromatin proteins are those that require intact DNA for their association with the nucleus and are released by 0.25 M ammonium sulfate after internucleosomal DNA is cut with DNAase I. The resulting structure retains most heterogeneous nuclear ribonucleoprotein (hnRNP) and is designated the RNP-containing nuclear matrix. The proteins of hnRNP are those associated with the nucleus only if RNA is intact. These are released when nuclear RNA is briefly digested with RNAase A. Ribonuclease digestion releases 97% of the hnRNA and its associated proteins. These proteins correspond to the hnRNP described by Pederson (Pederson, T., 1974, *J. Mol. Biol.*, 83:163–184) and are distinct from the proteins that remain in the ribonucleoprotein (RNP)–depleted nuclear matrix. The RNP-depleted nuclear matrix is a core structure that retains lamins A and C, the intermediate filaments, and a unique set of nuclear matrix proteins (Fey, E. G., K. M. Wan, and S. Penman, 1984, *J. Cell Biol.* 98:1973–1984). This core had been previously designated the nuclear matrix–intermediate filament scaffold and its proteins are a third, distinct, and nonoverlapping subset of the nuclear nonhistone proteins.

Visualizing the nuclear matrix using resinless sections shows that nuclear RNA plays an important role in matrix organization. Conventional Epon-embedded electron microscopy sections show comparatively little of the RNP-containing and RNP-depleted nuclear matrix structure. In contrast, resinless sections show matrix interior to be a three-dimensional network of thick filaments bounded by the nuclear lamina. The filaments are covered with 20–30-nm electron dense particles which may contain the hnRNA. The large electron dense bodies, enmeshed in the interior matrix fibers, have the characteristic morphology of nucleoli. Treatment of the nuclear matrix with RNAase results in the aggregation of the interior fibers and the extensive loss of the 20–30-nm particles. This RNP-depleted nuclear matrix is markedly distorted in overall shape when compared to the RNP-containing nuclear matrix.

COMPARED to the detailed knowledge of the arrangements of defined sequences within DNA, little is known of its organization in the nucleus. The interior of the eukaryotic nucleus and its composition has been particularly difficult to study. There is strong evidence of a nuclear skeleton or matrix, but its nature and even its existence has been the subject of conflicting reports (4). Biochemical analysis of nuclear structure has been hampered by the absence of reliable morphological studies. Conventional methods of electron microscopy fail to image the protein fiber networks that comprise the nonchromatin portion of the nucleus. In this report we use a resinless section technique for electron microscopy of the purified nonchromatin nuclear interior. In conjunction with the improved microscopy technique, we have developed a procedure that separates the chromatin, heterogeneous nuclear ribonucleoprotein (hnRNP),[1] and nuclear matrix with great precision while preserving the morphology of the nuclear matrix. The exper-

1. *Abbreviations used in this paper:* CSK, cytoskeleton; DGD, diethylene glycol distearate; hnRNA, heterogeneous nuclear RNA; hnRNP, heterogeneous nuclear ribonucleoprotein; LIS, lithium diiodosalicylate; n-BA, *n*-butyl alcohol; NM-IF, nuclear matrix–intermediate filament; RNP, ribonucleoprotein.

iments show that nuclear RNA has a role in organizing the matrix structure.

Early studies of nonchromatin nuclear structure were morphological. Since conventional electron micrographs do not show nuclear components other than chromatin, Bernhard and co-workers developed the EDTA regressive stain for nuclear studies. These studies suggested non-nucleolar fibrillogranular ribonucleoprotein (RNP) domains in interchromatinic regions of the nucleus (9, 10, 42, 51, 59). High resolution autoradiography showed labeled nuclear RNA in these fibrillogranular domains (19, 20, 44). The data showed that perichromatinic granules and fibrils near the borders of condensed chromatin contain both nascent and steady-state RNA.

More recent studies of nuclear structure have largely used biochemical fractionation to separate chromatin from the nuclear matrix. Most preparations begin with isolated nuclei, and chromatin is removed by exposure to high salt (2 M NaCl) followed by nuclease digestion (5–7, 12, 16, 24). Alternatively, the detergent lithium diiodosalicylate (LIS) and EDTA have been used with some cell types to render chromatin accessible to DNAase digestion (41). These procedures produce a matrix with much of the heterogeneous, nuclear RNA (hnRNA) still bound (34, 37, 40, 53, 61). Histones are removed in these procedures causing the chromatin to extend as DNA loops that remain firmly attached to the matrix at sites corresponding to DNA replication points (7, 33, 39, 41, 47, 62). Steroid receptor binding sites are found on the matrix (2, 17), and some actively transcribed genes are preferentially associated with this matrix (15, 18, 31, 38, 41, 45, 52, 53, 55).

A different strategy for removing chromatin from the nuclear matrix is used in the combined morphological and biochemical studies reported here. Several important nuclear constituents are preserved in the final preparation. In particular, the proteins of hnRNP, lost in the 2 M NaCl extraction (11), are retained. Several reports of an RNA constituent of nonchromatin nuclear structure have appeared (3, 12, 16, 26, 32, 35, 40, 43, 51). This report shows that chromatin removal is possible without disrupting the RNP-filament domains, and suggests they are essential to nuclear matrix organization (26, 32).

Materials and Methods

HeLa Cells

Suspension HeLa cells (S3) were grown in spinner bottles at 37°C in Eagle's minimum essential medium supplemented with 7% horse serum (Irvine Scientific, Santa Ana, CA). Cells were maintained at 4×10^5 cells/ml.

Cell Labeling and Fractionation

HeLa cells were pelleted at 650 *g*, washed in PBS, and resuspended in Eagle's medium that lacked either lysine or methionine. Protein was pulse-labeled at 37°C with 10 μCi/ml L-[4,5-^{3}H (*N*)]lysine (1 mCi/ml, 64.5 Ci/mmol), or 25 μCi/ml L-[^{35}S]methionine (8.3 mCi/ml, 1,064 Ci/mmol) for 2 h or 1 h, respectively. hnRNA was labeled, after a 30-min preincubation in 0.05 μg/ml actinomycin D, for 10 min in 10 μCi/ml [5-^{3}H]uridine (1 mCi/ml, 26.8 Ci/mmol). DNA was labeled for 12 h in 10 μCi/ml [methyl-^{3}H]thymidine (1 mCi/ml, 20.0 Ci/mmol). All radiochemicals were obtained from New England Nuclear (Boston, MA).

Cells were washed with phosphate-buffered saline (PBS) (4°C) as above. Pellets were resuspended in cytoskeleton (CSK) buffer (100 mM NaCl, 300 mM sucrose, 10 mM Pipes [pH 6.8], 3 mM $MgCl_2$, 1 mM EGTA, 1.2 mM phenylmethylsulfonyl fluoride, 2 mM vanadyl adenosine, and 0.5% Triton X-100) and incubated at 4°C for 3 min. Skeletal frameworks were pelleted after centrifugation at 650 *g* for 5 min and the supernatant, which contained soluble proteins, was removed. An extraction buffer (250 mM ammonium sulfate, 300 mM sucrose, 10 mM Pipes [pH 6.8], 3 mM $MgCl_2$, 1 mM EGTA, 1.2 mM phenylmethylsulfonyl fluoride, 2 mM vanadyl adenosine, and 0.5% Triton X-100) was added to the skeletal framework for 5 min at 4°C. The eluted protein were removed in the supernatant after centrifugation as above.

The chromatin fraction was removed from the remaining structure after digestion for 20 min at 20°C in a buffer identical to the CSK buffer but containing only 50 mM NaCl and 100 μg/ml bovine pancreatic DNAase I (EC 3.1.4.5, Worthington Biochemical Corp., Freehold, NJ). DNAase I was purified according to the method of Wilchek and Gorecki (63). Digestion in DNAase I was terminated by addition of ammonium sulfate to a final concentration of 0.25 M. The nuclear matrix was pelleted at 1,000 *g* for 5 min and the chromatin fraction removed in the supernatant. RNA and associated proteins were released from the nuclear matrix after digestion with 25 μg/ml RNAase A (EC 3.1.4.2, Sigma Chemical Co., St. Louis, MO) in CSK buffer (vanadyl adenosine was omitted from this buffer) for 10 min at 20°C. The RNP-depleted nuclear matrix–intermediate filament (NM–IF) fraction was pelleted and the nuclear RNP was removed as a supernatant.

Electron Microscopy

HeLa cells were fractionated to various points in the protocol as described. Fractionated structures were fixed in 2% glutaraldehyde in CSK buffer for 30 min at 4°C. The fixed structures were washed three times in 0.1 M sodium cacodylate, pH 7.2 (10 min/wash, 4°C) and postfixed with 1% OsO_4 in 0.1 M sodium cacodylate for 5 min at 4°C and subsequently washed in 0.1 M sodium cacodylate. The structures were dehydrated through a series of increasing ethanol concentrations that ended with three changes of 100% ethanol. Structures were immersed in *n*-butyl alcohol (n-BA)/ethanol (2:1) then in nBA/ethanol (1:2) followed by four changes in 100% n-BA for 15 min each. The structures were transferred to diethylene glycol distearate (DGD, Polysciences, Inc., Warrington, PA) through a series of n-BA/DGD mixtures of 2:1 then 1:2 for 10 min each at 60°C followed by three changes of 100% DGD, 1 h each. Embedded structures were allowed to solidify, and DGD blocks were cut using glass knives at an angle of 10° on an MT-2B Porter-Blum ultramicrotome. Sections were placed on parlodion- and carbon-coated grids. DGD was removed by immersing grids in 100% n-BA at 23°C (three washes, 1 h/wash). The grids were returned to 100% ethanol through a granded series of ethanol/n-BA mixtures and dried through the CO_2 critical point. Sections were examined in a JEOL EM 100 B electron microscope at 80 kV.

hnRNP Preparation

hnRNP particles were prepared according to the protocol of Kish and Pederson (35). Briefly, HeLa cells were treated with 0.04 μg/ml actinomycin D for 30 min. Cells were transferred to medium containing [^{35}S]methionine (as described above) in the presence of 0.04 μg/ml actinomycin D. Cells were homogenized in reticulocyte standard buffer (RSB) (10 mM Tris-Cl, pH 7.2, 10 mM NaCl, 15 mM $MgCl_2$, 2 mM vanadyl adenosine, and 1.2 mM phenylmethylsulfonyl fluoride). Nuclei were disrupted by brief sonication. The sonicate was layered over a discontinuous sucrose gradient (4 ml of 60% sucrose, 1 ml of 45% sucrose, and 3 ml of 10% sucrose, all in RSB), and centrifuged in the Beckman SW40.1 rotor for 90 min at 26,000 rpm (Beckman Instruments, Inc., Palo Alto, CA). The hnRNP particles were recovered as a narrow opalescent band in the 45% sucrose layer.

Electrophoresis and Immunoblots

Histone proteins were examined on a 15% polyacrylamide gel prepared according to the method of Laemmli (36). Two-dimensional gels were prepared using equilibrium isoelectric focusing gels in the first dimension (47). Isoelectric points were determined using a calibration standard (pI range 4.7–10.6) provided by BDH Chemicals Ltd. (Poole, England). Immunoblots were prepared after transfer of proteins to nitrocellulose paper according to the method of Towbin et al. (60). Antibodies to cytokeratins were obtained from Labsystems (Helsinki, Finland). Antibodies to vimentin and lamins A and C were generously provided by Drs. R. O. Hynes and L. Gerace, respectively. Goat anti-rabbit, anti-mouse, and anti-guinea pig IgG conjugated to horseradish peroxidase was obtained from Cappel Laboratories (Cochranville, PA). Protein bands were visualized according to the method of Hawkes et al. (30).

Results

Nuclear Morphology

Resinless Section Microscopy of Intact and Detergent-extracted Nuclei. Resinless sections of intact cells reveal a wealth

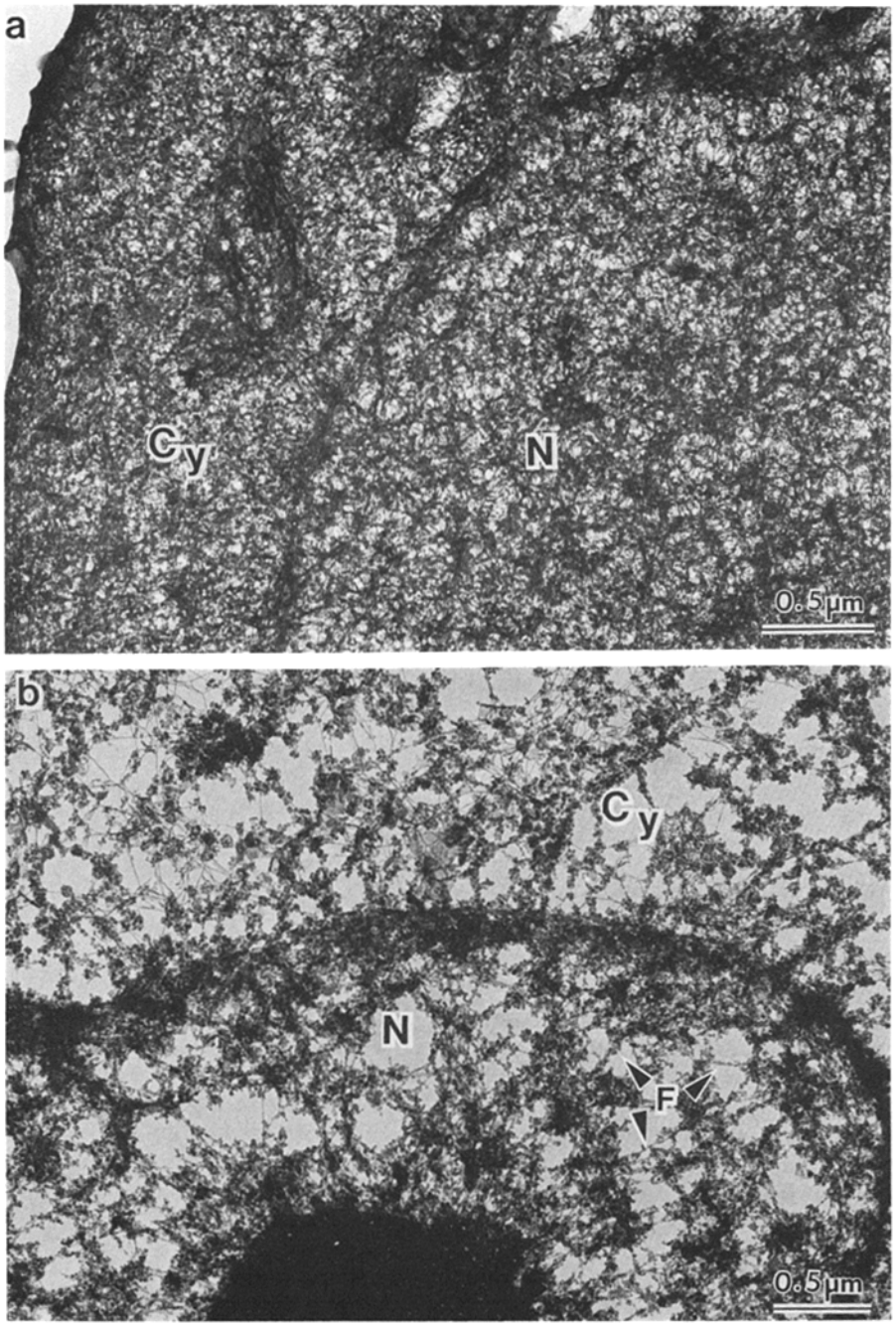

Figure 1. Transmission electron micrographs comparing an intact HeLa nucleus with a HeLa nucleus after extraction with Triton X-100. Intact cells (*a*) and cells extracted with Triton X-100 (*b*) were prepared as unembedded sections as described in the Materials and Methods. The intact nucleus (*a*), seen in a 0.2-μm section, appears as a microtrabecular structure as described by Porter (29, 64). The extracted nucleus (*b*) is a component of the skeletal framework, the structure that remains after phospholipid and >70% of the cellular protein is removed (13, 14, 23). The extracted nucleus is less dense than the intact nucleus, yet aspects of differentiated chromatin organization are clearly retained in this structure (see Fig. 6). A fibrillogranular network (*F*) is observed throughout the extracted nucleus. The cytoplasm (*Cy*) and the nucleus (*N*) are indicated in each micrograph.

of nuclear structure obscured in conventional embedded sections (13). The nuclear interior of an intact HeLa cell, shown in Fig. 1 *a*, consists of a dense lattice comprised of all the nuclear constituents, which include nonstructural nuclear proteins. As previously reported, this lattice resembles the microtrabeculae found in the cytoplasm of unextracted cells (29). However, this structure does not correspond to the usual definition of a purified nuclear matrix (2–8, 12, 15, 16, 18, 24, 31, 33, 34, 37–41, 45, 47, 52, 53, 55, 61, 62). Here, we use the term nuclear matrix to refer to the purified, isolated, nonchromatin nuclear structure.

The preparative procedure for the nuclear matrix described here affords subfractions of the nucleus with distinct compositions and also preserves overall nuclear morphology. The first step in the present experiments is to prepare the cytoskeletal framework using detergent extraction (14, 23, 57). This extraction removes phospholipids and the soluble cell proteins (70%). Consequently the microtrabecular lattice disappears, which reveals the underlying skeletal framework. Fig. 1 *b* shows a resinless section micrograph of a HeLa cell nucleus after soluble proteins have been removed. The dense trabecular lattice, seen in Fig. 1 *a*, is no longer present. Instead, there is a clear, detailed image of nuclear structure. The section reveals the fine structure of chromatin and nonchromatin fibers not seen in conventional embedded sections (see below) or when the microtrabecular lattice is present (Fig. 1 *a*). Filaments are visible in the diffuse euchromatinic regions and are continuous with the perichromatin filaments. Some of these

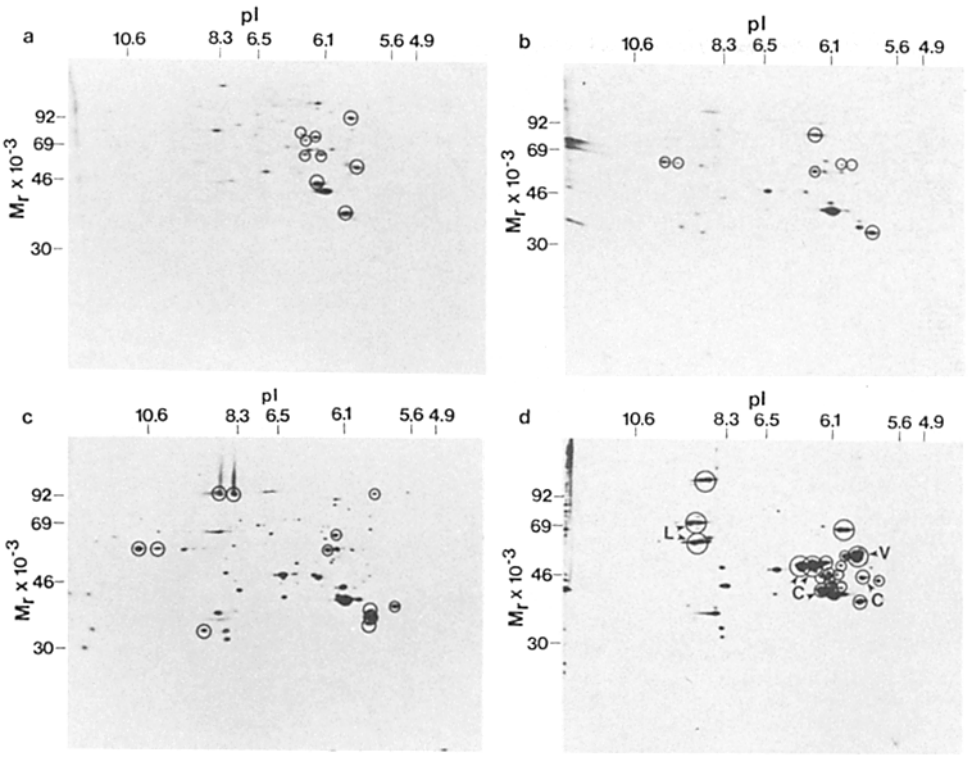

Figure 2. Analysis of proteins in individual nuclear fractions using two-dimensional gel electrophoresis. HeLa cells were labeled with [^{35}S]methionine for 1 h at 37°C and fractionated as described in Materials and Methods. Protein was concentrated by precipitation in acetone and aliquots that contained 200,000 cpm and were separated by equilibrium gel electrophoresis (46). Marker proteins (vimentin, *V*; lamins A and C, *L*; cytokeratins, 44, 46, 52, and 54 kD, *C*; actin, arrow) were determined by two-dimensional immunoblot analysis using appropriate antibodies (data not shown). Proteins that are represented predominantly in one fraction are circled. The protein fractions are those eluted by the initial salt elution (*a*), the chromatin proteins (*b*), the proteins released by RNAase A digestion (*c*), and the proteins of the RNA-depleted nuclear matrix (*d*).

nuclear components are shown below to correspond to RNP structures previously suggested by differential nuclear staining (19, 20, 51).

Sequential Fractionation of the Nucleus

Purification of the Nucleus. The skeletal framework, obtained by detergent extraction in physiological buffer, is extracted with double detergent (32) or with buffered 0.25 M ammonium sulfate. The two methods are essentially equivalent. Electron micrographs show the extraction effectively removes protein structures exterior to the nucleus with the exception of the intermediate filaments (23). The solubilized proteins (Fig. 2*a*) are largely from the cytoplasm and constitute a unique subset of cellular proteins (21, 23). Few proteins in this fraction are shared with the remaining nuclear fractions described below. The intermediate filaments have been shown to remain associated with both intact nuclei (56) and to extracted matrix preparations (14, 21, 23, 57) and are not found in extracted fraction.

Separation of Chromatin from the Nucleus. In the next step, DNA and the associated chromatin proteins are separated from the nucleus. The structure that remains contains most of the hnRNP and is designated the RNP-containing nuclear matrix. Our experiments show that high ionic strength (2 M NaCl), used to remove histones before digestion of chromatin, significantly alters the interior nuclear morphology (Fig. 9). A different strategy is used in the procedure described here. Chromatin is first digested with purified DNAase I in physiological buffer (100 mM NaCl, 10 mM Pipes [pH 6.8], 3 mM $MgCl_2$). The digestion cuts principally the DNA between the nucleosomes. Ammonium sulfate is then added to a concentration of 0.25 M. Chromatin is eluted in the form of intact nucleosomes. Vanadyl adenosine is present to inhibit ribonuclease activity and prevent hnRNA degradation.

Table I. Percent Distribution of Nuclear Components after Fractionation

Fraction	Protein*	hnRNA‡	DNA§
Chromatin	70	24	94
Nuclear-RNP	4	73	4
NM-IF	26	3	2

* Protein was determined on the basis of labeling with [^{35}S]methionine as described.

‡ hnRNA was measured by pulse labeling with [^{3}H]uridine in the presence of 0.04 μg/ml actinomycin D as described.

§ DNA was measured after labeling cells with [^{3}H]thymidine for 12 h as described.

The elution removes the nucleosomes and associated proteins that have been freed by DNA cleavage. The chromatin fraction contains 94% of the DNA, greater than 95% of the histones and 70% of the nonhistone nuclear proteins (Table I). To follow the partition of histones during fractionation, cells were labeled for 2 h with [^{3}H]lysine and fractionated. The lysine-labeled nuclear proteins were analyzed on a 15% polyacrylamide gel. The electropherogram in Fig. 3 shows that the first exposure to ammonium sulfate, before digestion with DNAase, releases histone H1, but the core histones remain with the nucleus. Subsequent elution with 0.25 M ammonium sulfate after the DNase I digestion releases >95% of the core histones in the chromatin fraction.

In addition to the histones, the fractionation separates a distinct subset of chromatin proteins (Fig. 2*b*) from the other nuclear fractions. There are almost no chromatin protein spots (Fig. 2*b*), apart from actin, corresponding to proteins of the nuclear RNP complex (Fig. 4*c*) or of the RNP-depleted nuclear matrix (previously termed NM-IF [23]) (Fig. 2*d*). Fig. 2*a* shows the proteins removed by the extraction with 0.25 M ammonium sulfate. None of these proteins, with the

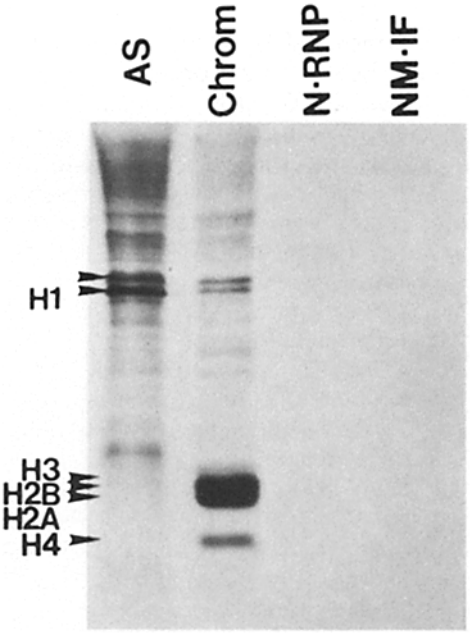

Figure 3. Localization of histones in the nuclear fractions. HeLa cells were labeled for 2 h with [^{3}H]lysine and fractionated as described in Materials and Methods. Protein fractions from 2 × 10^7 cells were separated by gel electrophoresis on a 15% polyacrylamide gel (36). Histones were identified on the basis of molecular weight and preferential labeling with lysine. The majority of the core histones (>95%) were localized in the chromatin fraction (*Chrom*). Fewer than 5% of the core histones were released in the initial elution with ammonium sulfate (*AS*). The initial salt elution released a significant proportion of histone H1. Trace amounts of histones were observed in the nuclear RNP (*N-RNP*) and the RNP-depleted nuclear matrix (*NM-IF*) fractions.

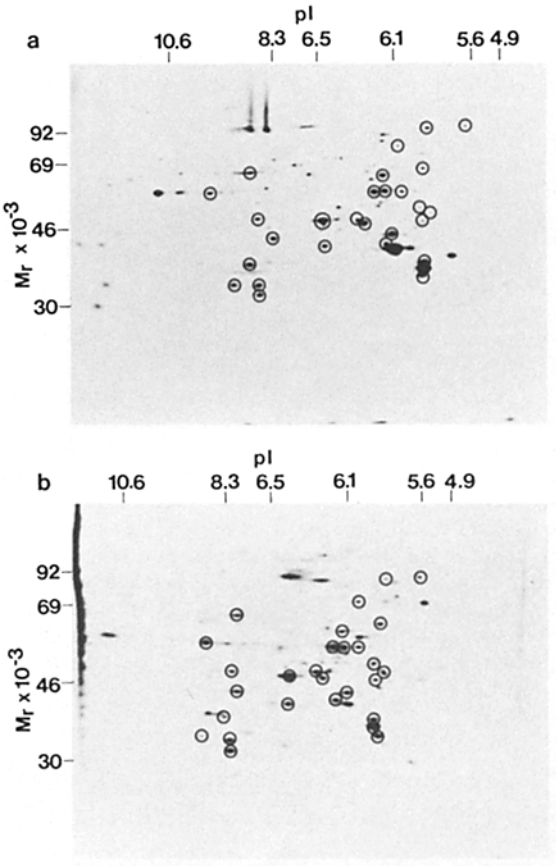

Figure 4. Comparison of proteins released by treatment with RNAase with hnRNP proteins obtained from a standard preparation. HeLa nuclear proteins released by treatment with RNAase (*a*) were obtained as described in Fig. 2. hnRNP complexes (*b*) were isolated according to the method of Pederson (48). Proteins (200,000 cpm/fraction) were separated by two-dimensional gel electrophoresis (46). The nuclear RNP (*a*) were compared with proteins obtained from a preparation of hnRNP obtained after sucrose gradient separation of a nuclear sonicate (*b*). Proteins in the nuclear RNP fractions (*a*) that are common to the hnRNP fraction (*b*) are indicated by circles. A majority of proteins observed in the hnRNP fraction are also components of the RNP-containing nuclear matrix.

exception of actin, are present in the chromatin fraction. Histones are not focused on these equilibrium gels. The most abundant nonhistone chromatin protein spots (Fig. 2*b*) are actin (arrow) and an unknown acidic protein. There are ~30 chromatin proteins of intermediate abundance. The distinct patterns of the proteins from each nuclear fraction argues strongly against random precipitation artifacts or significant cross-contamination during the preparation of the nuclear matrix.

Proteins of the Nuclear RNP. The RNP filaments of the matrix are an important component of matrix architecture. A brief digestion of the RNP-containing matrix with RNAase A removes 97% of the hnRNA (Table I). Consequently, proteins associated with the matrix by RNA are released quantitatively. These proteins, referred to here as nuclear RNP, comprise ~4% of the total nuclear protein (Table I).

Figs. 2*c* and 4*a* show two-dimensional gel electropherograms of proteins from the nuclear RNP fraction. The gels have ~30 major protein spots that are predominantly >30 kD and have a wide range of isoelectric points. The pattern shares few proteins of the chromatin fraction shown in Fig. 2*b*. Circles mark those major proteins detectable in only one fraction. These RNP proteins were compared with those in the nuclear RNP preparation of Pederson (48). RNP particles were prepared from labeled nuclei by sonication. The particles were purified by sedimentation in a sucrose density gradient and proteins analyzed by two-dimensional gel electrophoresis (Fig. 4*b*). The proteins of the Pederson RNP particle are largely >30 kD. More than 90% of the Pederson proteins are the same as the RNP proteins obtained here (Fig. 4*a*).

Proteins of the RNP-depleted Nuclear Matrix or NM-IF. Fig. 2*d* shows a two-dimensional electropherogram of the proteins of the RNP-depleted nuclear matrix. The pattern shows no significant overlap with chromatin or RNP proteins. Most of the matrix proteins are unique to this fraction. These include lamins A and C, the cytokeratins, and vimentin. Immunoblots were used to localize several major proteins in the matrix. The nuclear fractions from 10^7 HeLa cells were analyzed on a 10% polyacrylamide gel. The gel patterns were transferred to nitrocellulose and incubated with the appropriate antibodies. Fig. 5 shows the blots of cytokeratins (Fig. 5*a*), vimentin (Fig. 5*b*), and lamins A and C (Fig. 5*c*). Arrows indicate the lamins A and C, cytokeratins, and vimentin in Fig. 2*d*. Greater than 95% of each of the protein species analyzed were localized in the RNP-depleted nuclear matrix (NM-IF). The RNP-depleted nuclear matrix contains a few

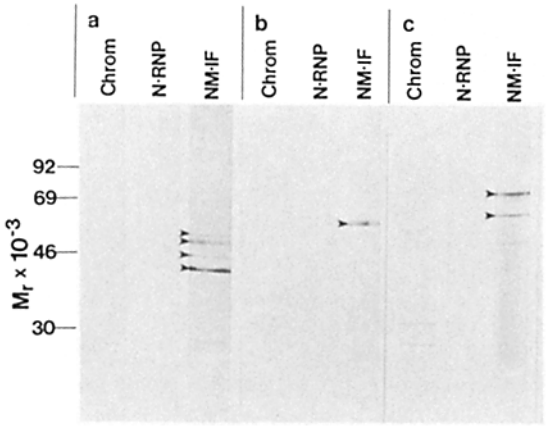

Figure 5. Immunoblot localization of lamins A and C, vimentin, and the cytokeratins in the NM-IF scaffold. HeLa cells (5×10^6) were fractionated as described in Materials and Methods. Proteins from each of the nuclear fractions were separated on 10% polyacrylamide gels and transferred to nitrocellulose strips. The strips were incubated with antibodies to vimentin (*a*), cytokeratins (*b*), and lamins A and C (*c*), and processed as described. In each reaction, the antigen was observed predominantly in the RNP-depleted nuclear matrix fraction (*NM-IF*). At this level of sensitivity, no antigen was detectable in either the chromatin (*Chrom*) or RNAase released nuclear RNP fractions (*N-RNP*).

abundant proteins and a complex set of minor ones. The many minor spots in Fig. 2*d* change markedly in different cell types.

Morphology of the Nucleus and Nuclear Matrices

Electron Microscopy of the Sequential Fractionation: Conventional Epon-embedded and Resinless Sections. The biochemically precise nuclear fraction make corresponding specific contributions to nuclear morphology. Fig. 6 shows nuclear morphology at the different steps. Fig. 6 shows both the conventional Epon-embedded sections (*a*, *c*, and *e*) and the resinless section images (*b*, *d*, and *f*) of the nuclear preparations. Fig. 6, *a* and *b* show the original nucleus of the skeletal framework, Fig. 6, *c* and *d*, the nuclear structure with only chromatin removed (RNP-containing matrix), and Fig. 6, *e* and *f*, the nuclear matrix with the nuclear RNA removed (RNP-depleted nuclear matrix).

The conventional Epon section of the HeLa nucleus (Fig. 6*a*) shows relatively few cytoplasmic fibers (14, 64) and little nonchromatin nuclear structure. Such sections do indicate that the extraction with physiological ionic strength and pH of the CSK buffer preserves overall cytoskeleton and nuclear morphology. The nuclei retain the distinct regions of chromatin organization. The Epon section shows clearly the central and marginal heterochromatin masses (*H*) interspersed with regions of euchromatin (*E*) and perichromatin (*P*). The heavily stained nucleolus (*Nu*) is easily identified.

The embedment-free image of cytoskeletal framework (Fig. 6*b*) shows more clearly the protein filament networks of the cytoplasm and nucleus. Networks of fine filaments extend throughout the nucleus and terminate at the nuclear lamina (arrows; Fig. 6*b*). Filamentous structures are visible in the diffuse euchromatinic regions and are continuous with the perichromatin filaments. These nuclear components probably correspond to structures previously suggested by differential nuclear staining (19, 20, 51).

It is important that, in these and the following micrographs, the appropriate comparison be made between Epon-embedded and resinless sections. It might seem simplest to compare sections of similar thickness. Actually, the modes of imaging are so different that equivalency is difficult to define or establish. This will be considered further in the Discussion. The section thicknesses used in these micrographs probably offer the most meaningful comparisons between the two different methods of electron microscopy.

Morphology of the RNP-containing Nuclear Matrix. The DNAase digestion and salt elution leave the RNP-containing nuclear matrix almost free of chromatin. Most of the hnRNA (80%) remains tightly associated with this structure (Table I). A future report will show that this bound hnRNA is a subset of total nuclear RNA sequences and is specifically and tightly associated with the matrix (Fey, E. G., and S. Penman, manuscript in preparation). Fig. 6*c* shows the morphology of the RNP-containing matrix in a conventional Epon-embedded section and Fig. 6*d* the image in a resinless section. The Epon section is typical of earlier micrographs of chromatin-depleted nuclear structures. It shows principally a thin lamina surrounded by fragments of cytoplasmic filaments. The nuclear interior shows only some fragments of filaments and a heavily stained nucleolus (*Nu*).

The resinless sections offer a much clearer view of the interior of the RNP-containing matrix. The sections are thin (0.2 μm) compared to the HeLa cell nucleus (10 μm) so that few sections are tangential to, and therefore show, the surface of the dense nuclear lamina. Figs. 6*d* and 7 show the interior of the RNP-matrix to be rich in filament networks. A set of 10-nm filaments exterior to the nuclear lamina boundary (*L*) are probably intermediate filaments of vimentin and keratin (25). The stereoscopic view in Fig. 7 shows these terminate directly on the nuclear lamina.

In sharp contrast to the conventional section (Fig. 6*c*) in which the nuclear interior appears empty, the resinless section (Fig. 6*d*) reveals the RNP-containing nuclear matrix interior to be filled with an anastomosing network of filaments. Dense clusters of electron opaque 25–30-nm granules, associated with the fibers, are now visible (*P*; Fig. 5, *c* and *d*). These 25–30-nm granules correspond in size to the RNP particles described by several laboratories (11, 49, 50, 54). The nucleoli (*Nu*, Fig. 6*c*) are large, dense bodies enmeshed in the nuclear matrix filaments. The interior morphology of the nucleoli is visible in sufficiently thin sections ($\leq$0.2 μm). Fig. 6*d* shows the familiar nucleolar structure of dense, coiled fibrils surrounded by granular regions. Some empty regions appear in the matrix fiber network that may result from tearing during sectioning.

A powerful feature of embedment-free electron microscopy is that it images the entire contents of a sample and not just the stained surface of a section. Consequently, the resinless sections offer striking stereoscopic views of three-dimensional organization that can be obtained no other way. Fig. 7 shows a stereoscopic micrograph of a 0.2-μM section of the RNP-containing matrix taken at 5° (±) tilt angles. The stereoscopy shows the lamina (*L*) to be a spherical shell with cytoplasmic filament fibers that terminate throughout its exterior surface. The nuclear interior contains a dense nucleolus (*Nu*) held

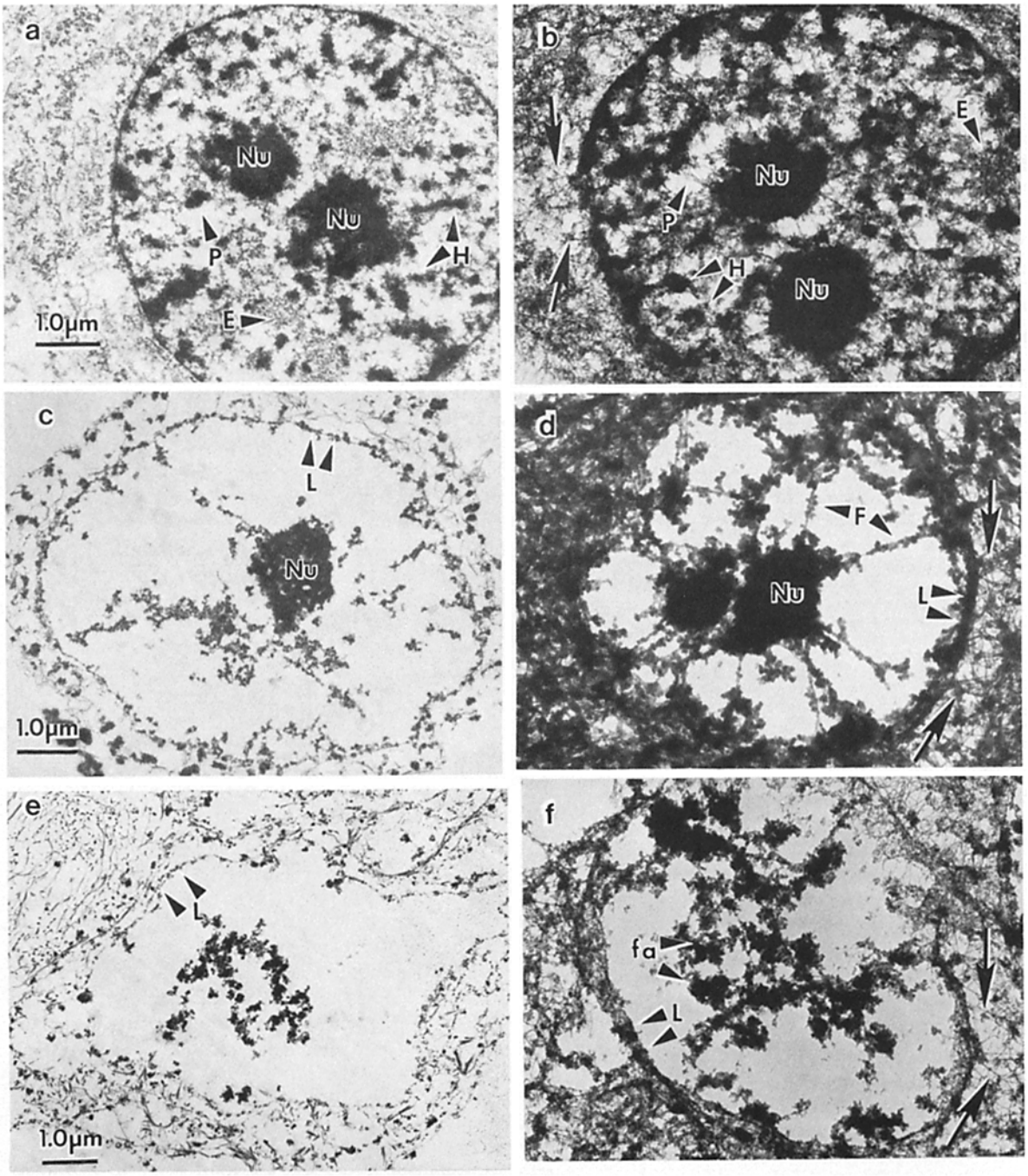

Figure 6. Transmission electron micrographs comparing fractionated HeLa nuclei in Epon-embedded sections and in unembedded resin-free sections. Nuclei obtained after extraction with Triton X-100 (*a* and *b*), RNP-containing nuclear matrices (*c* and *d*), and RNP-depleted nuclear matrices (*e* and *f*) were prepared as described in Materials and Methods. Nuclear preparations were fixed in glutaraldehyde, postfixed in OsO_4, and embedded either in Epon-Araldite (*a*, *c*, and *e*) or the removable embedding compound DGD (*b*, *d*, and *f*). The organization of chromatin is seen after extraction with Triton X-100 (*a* and *b*). The retention of differentiated regions of heterochromatin (*H*), euchromatin (*E*), and nucleoli (*Nu*) is observed in both sections. Detail of filaments in the perichromatinic space (*P*) and the association of cytoplasmic filaments with the nuclear lamina (arrows) are observed only in the unembedded image (*b*). Chromatin and associated proteins were removed as described, and the resulting RNP-containing nuclear matrix (*d*) revealed a dense interior matrix of fibers (*F*) that extends throughout the nucleus, forming continuous associations between nucleoli and the nuclear lamina (*L*). Cytoplasmic filaments were again observed in association with the nuclear lamina (arrows) only in the unembedded section (*d*). The detail and continuity of structural elements in the RNP-containing nuclear matrix interior is masked in the embedded section (*c*). Nuclear RNA was removed with ribonuclease A, and the RNP-depleted nuclear matrices were examined as above. Both the embedded (*e*) and unembedded (*f*) sections display a distortion of nuclear shape. The interior of the nuclear matrix, after digestion with ribonuclease, is composed of large filament aggregates (*fa*). These structures are larger than the filaments (*F*) seen in *d*. These aggregates appear condensed and fragmented. Both the loss of gross nuclear shape and the distortion of the interior by digestion with RNAase suggest that RNA is an important structural component of the nucleus. Epon-embedded sections (*a*, *c*, and *e*) are 0.05-μm thick; unembedded sections (*b*, *d*, and *f*) are 0.2-μm thick.

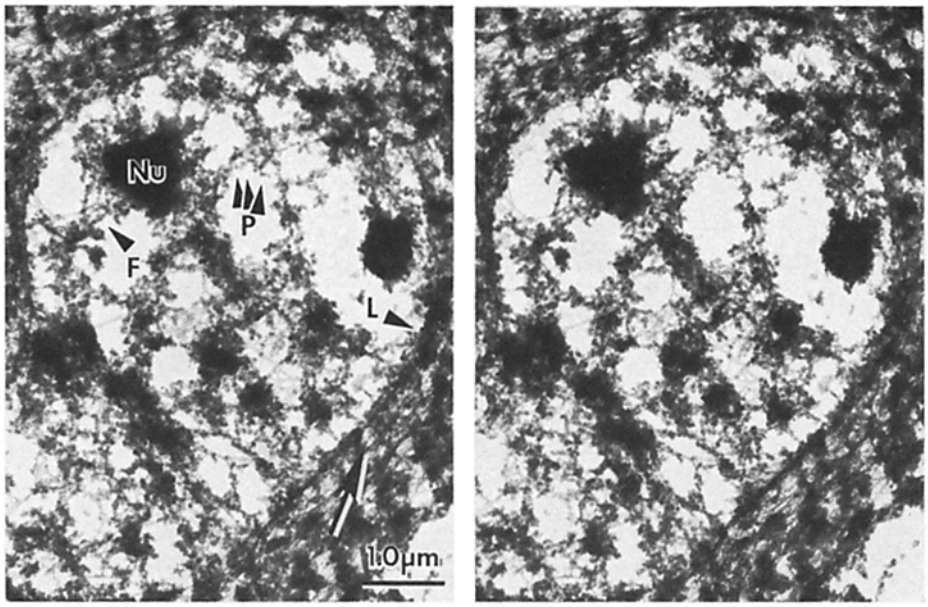

Figure 7. Stereo transmission electron micrograph of the RNA-containing nuclear matrix. The RNA-containing nuclear matrix was prepared as described in Fig. 5. Sections (0.2-μm thick) were examined in stereo at a total tilt of 10° (+ and −5°). The stereo image demonstrates that this preparation is not collapsed. The RNA-containing nuclear matrix is seen as a self-supporting three-dimensional structure. The nuclear lamina (*L*) is an extended sheet that divides the three-dimensional domain of the nuclear interior from the cytoplasm. Filaments in the cytoplasm (arrows) terminate at the surface of the nuclear lamina. The fibers (*F*) inside the nucleus are studded with 25–30-nm particles (*P*) and appear as an ordered network that connects the nucleolus (*Nu*) with the convex surface of the lamina.

apparently suspended in position by a dense network of matrix filaments.

Altered Morphology of the NM-IF. The RNP-depleted nuclear matrix, with the associated intermediate filaments, remains after the removal of chromatin and hnRNP. We have previously designated this structure the NM-IF scaffold (21, 23) to denote the apparent role of the intermediate filaments in tissue architecture. The proteins of the RNP-depleted nuclear matrix constitute a third distinct subset of nuclear proteins and include all of the nuclear lamins (27, 28), vimentin, and cytokeratins (see below). The matrix is largely, although not entirely, free of remnant nucleic acids. It has <3% of initial DNA or RNA (see Table I).

A role of the nuclear RNP in determining matrix organization is revealed by the resinless section electron micrographs. Removing the nuclear RNA greatly alters the interior morphology of the nuclear matrix. Fig. 6, *e* and *f* show this RNP-depleted matrix (or NM-IF scaffold). Intermediate filaments remain associated with the cytoplasmic face of the nuclear lamina (arrows). The Epon section shows the interior fibers have been replaced by dark, amorphous aggregates. These aggregates are probably not remnant nucleoli. They are often larger than nucleoli, appear scattered throughout the nuclear space, and do not have a nucleolar morphology (Fig. 6, *b* and *d*). The nature of these aggregates is much clearer in the resinless sections.

Fig. 6*f* shows the resinless section image of the RNA-depleted matrix. The morphology is greatly altered from the RNP-containing nuclear matrix in Fig. 6*d*. Removal of hnRNP results in marked distortion of overall nuclear shape. A few dense aggregates replace large portions of the interior network of 20–30-nm filaments. Many of the 20–30-nm granules of the interior fibers of the RNP-containing nuclear matrix have been removed by the digestion, which suggests they contain RNA. The marked reorganization effected by RNAase indicates a role of nuclear RNP in organizing the nuclear interior.

The altered three-dimensional organization of the RNP-depleted nuclear matrix is shown best by stereoscopic electron microscopy (Fig. 8). Most fibers seen in the RNP-containing nuclear matrix (Fig. 7) have been replaced by dense aggregates. The image shows the unaltered connection of the nuclear matrix to the exterior intermediate filaments.

Morphology of the High Salt Matrix in Resinless Section Microscopy. The morphology of the RNP-containing nuclear matrix is very different from that of matrices prepared using 2 M NaCl (2–8). Fig. 9, *a* and *b* shows low and high magnification resinless section micrographs of the high salt matrix and compares them to the RNP-containing and RNP-depleted nuclear matrices obtained here. Fig. 9, *a* and *b* shows the interior fibers collapsed and possibly aggregated. The fine structure of these fibers is altered with many of the granules missing. The overall shape of high salt matrix is distorted, and the structure appears flaccid. These alterations may result from disruption of protein associations by the high ionic strength or by the mechanical stress caused by DNA distension. Since hnRNP has a role in nuclear structure, described above, the loss of the hnRNP proteins in 2 M NaCl (11) may also contribute to the altered morphology of the high salt preparation.

Discussion

The experiments reported here use, for the first time, resinless section microscopy to view the structures obtained by an improved, relatively nondisruptive fractionation of the nucleus. Used in concert, these techniques reveal the distinct substructures of the nucleus and their protein composition. One unexpected result is the role of nuclear RNA in the organization of the nuclear matrix.

Many structures masked in conventional electron microscope preparations are imaged by the resinless sections. Image formation results from differential electron scattering. The customary section techniques surround biological structure with plastic of nearly identical scattering power. Images are actually formed by heavy metal stains that scatter electrons more than the embedding resin. Without special staining procedures, conventional images are largely restricted to that

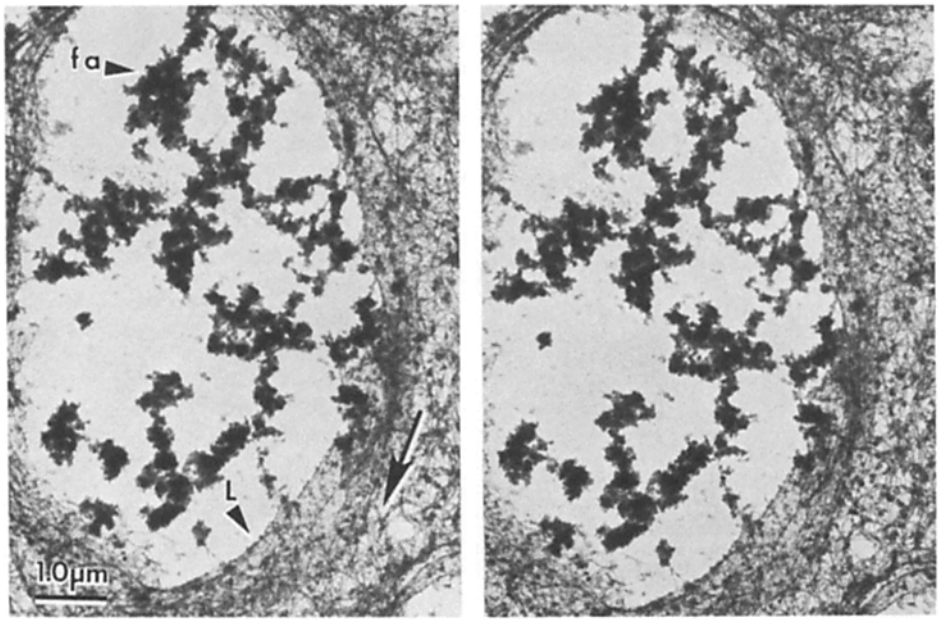

Figure 8. Stereo transmission electron micrograph of the RNA-depleted nuclear matrix. Sections (0.2-μm thick) of RNA-depleted nuclear matrix were examined in stereo (total tilt 10°, + and −5°). Although there is distortion of the structure of the nuclear in the NM–IF preparation, many aspects of three-dimensional cellular organization are retained. The lamina (*L*) retains an interaction with the system of cytoplasmic filaments (arrows) that has a regularity in three dimensions observed in the RNP-containing nuclear matrix structure (Fig. 6). The filament aggregates inside the nucleus (*fa*) show little structural regularity and have lost the connectedness characteristic of the filaments in the RNP-containing nuclear matrix.

portion of the sample at the section surface since heavy metal atoms do not penetrate dense plastic. Embedment-free techniques, such as the resinless sections, dispense with embedding resin, and images are formed directly by biological structure in vacuum (1). Fibers throughout a section are imaged, not just at the section surface, making stereoscopic microscopy a powerful adjunct of morphological analysis.

Section thickness has a very different significance in the two methods of microscopy. Embedded sections are usually made as thin as possible to minimize image degradation by electron scattering from the resin. The resinless section has no comparable source of image degradation and its thickness is chosen to give an appropriate number of objects in a field. Sections of similar thickness are not comparable since they image the section contents so differently.

The resinless section technique pioneered by Wolosewick (64) used polyethylene glycol as the temporary embedding medium. The procedure proved difficult in our hands and we developed the method based on DGD (13). This has proved convenient and well suited to the extracted samples studied here.

The resinless sections are well suited for monitoring steps in the matrix preparation. Conventional micrographs fail to image nonchromatin nuclear structure, while embedment-free whole mounts show mostly the exterior nuclear lamina (14, 23). The resinless sections shown here characterize the nuclear interior as composed largely of fibrillogranular networks. Their morphology is highly sensitive to RNAase, and the nuclear fractionation technique was modified to prepare the matrix both with and without its RNP component.

These micrographs show for the first time that treating the RNP-containing nuclear matrix with ribonuclease releases the RNP and has marked effects on its morphology. There is a large reduction in the number of 20–30-nm granules clustered on the interior matrix fibers. Most of the fibers collapse into dense aggregates leaving much of the nuclear volume empty. Before the removal of RNA, the RNP-containing nuclear matrix is ovoid and has the dimensions of a cell nucleus. RNAase digestion seems to destroy much of the mechanical stability of the matrix and it now appears flaccid and distorted. The results suggest that nuclear RNA plays a role in nuclear structure, either directly or through its associated proteins.

A major technical innovation used here is a much gentler method of removing chromatin from the nuclear matrix. Chromatin is notoriously recalcitrant and digestion with DNAase alone leaves most remaining in the nucleus. Previous procedures used high salt or strong detergent to strip the histones and render DNA accessible to DNAase. Upon removal of the histones, the DNA springs out into loops but the bases of the loops remain firmly attached to the matrix.

We found that by first cutting internucleosomal DNA in the native chromatin with DNAase, nucleosomes can be eluted by a moderate salt concentration (0.25 M ammonium sulfate). Histones are not released and no chromatin halo is produced. This reduced salt elution does not disrupt hnRNP complexes (26, 32), which retain their full complement of proteins. The fractionation is highly reproducible, insensitive to small variations in procedure, and applicable to a wide variety of cells. One reason for this reproducibility is that the fractions are not arbitrary or defined capriciously. They correspond to physical entities preexisting in the nucleus.

The very different physical properties of the RNP-depleted nuclear matrix, of hnRNP, and of chromatin permit unambiguous and meaningful separation of their proteins. Thus: (*a*) Chromatin proteins are those released only after digestion of internucleosomal DNA. The mild elution with 0.25 M ammonium sulfate is essential. The chromatin proteins are extracted only with both DNAase digestion and salt elution. Used alone, neither the salt nor the enzyme removes significant amounts of nuclear protein. (*b*) Nuclear RNP proteins are those released only by digestion of nuclear RNA. (*c*) The core RNP-depleted nuclear matrix (previously termed the NM–IF) consists of those proteins remaining after the removal of nucleic acids and their associated proteins. It is characteristically stable at high ionic strength. Removing the nuclear RNP profoundly affects the morphological organization of the nuclear matrix.

The nuclear fractions have unambiguously different protein

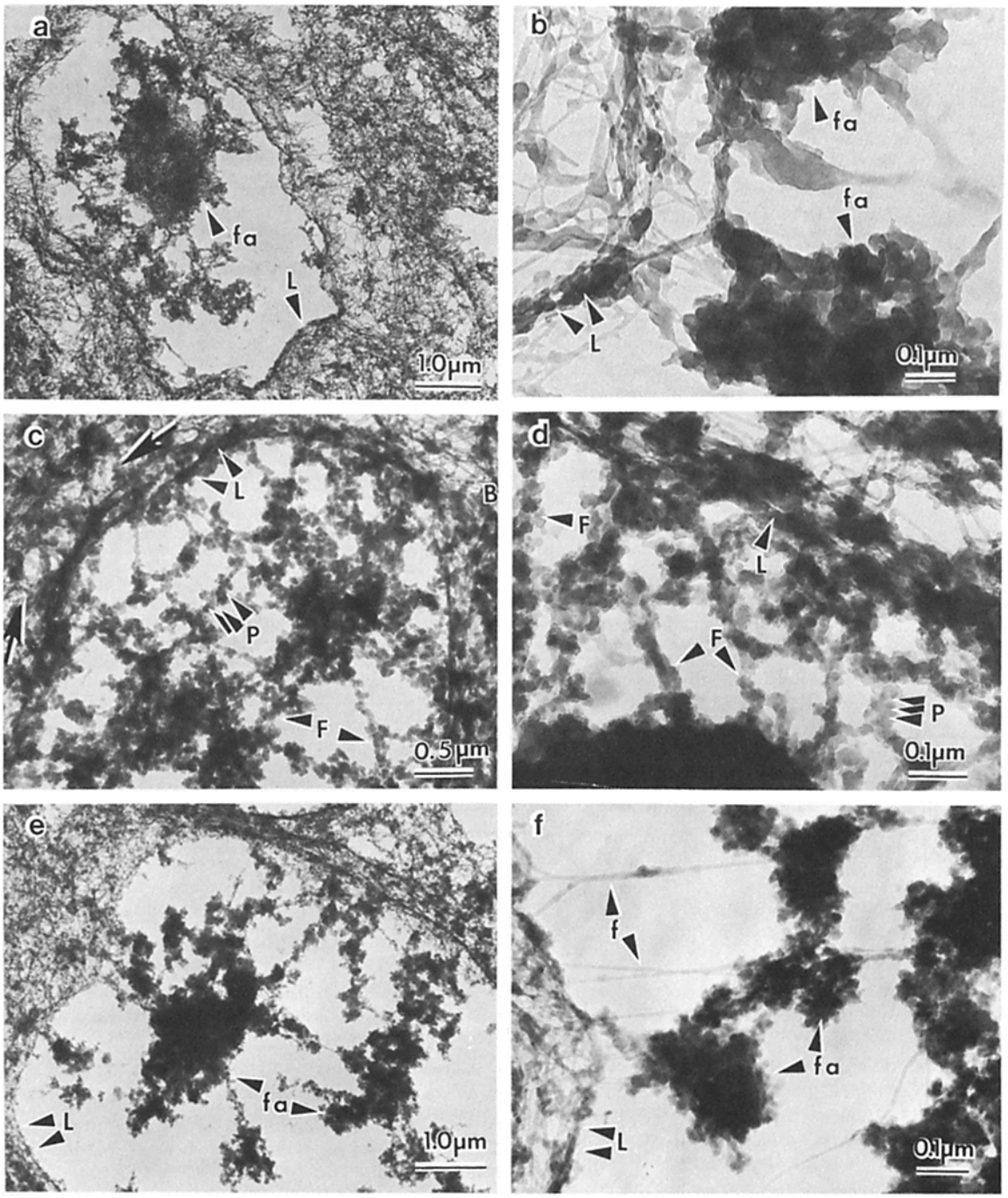

Figure 9. Transmission electron micrographs comparing the nuclear matrix derived using 2 M NaCl with the RNA-containing and RNA-depleted nuclear matrices. HeLa nuclei were prepared as described and incubated for 20 min at 20°C with 100 μg/ml DNase I. A portion of these nuclei were extracted with 2 M NaCl as described and the resulting nuclear matrices were examined (*a* and *b*). For comparison, RNP-containing (*c* and *d*) and RNP-depleted nuclear matrices (*e* and *f*) were prepared from identical nuclei. It is clear from these micrographs that the nuclear matrix prepared with 2 M NaCl (*a* and *b*) does not retain the fibrillogranular network observed in the RNA-containing nuclear matrix described here (*c* and *d*). The 2 M NaCl nuclear matrix (*a* and *b*) has dense aggregates throughout the nuclear interior. These aggregates are similar to those observed in the RNA-depleted nuclear matrix preparation (*e* and *f*). Lamina, *L*; 20–30 nm-particles, *P*; filaments, *F*; filament aggregates, *fa*.

compositions. Few proteins appear in more than one fraction. The absence of cross-contamination between the sets of nuclear proteins indicates that nonspecific precipitation is not significant during the fractionation. Most important is that the sequential fractionation is totally conservative. The procedure accounts for all proteins initially present; nothing is discarded. This conservation makes quantitative comparisons of the nuclear fractions possible.

The separate removal of nuclear RNP is an important modification of the previous moderate salt preparation (14). Formerly, RNA and DNA were digested together. The present procedure permits electron microscopy of RNP-matrix with

intact RNA. Some of the 20–30-nm granules in the complex probably contain this RNA. This additional step also yields RNP proteins in pure form for separate biochemical analysis.

The results reported here are significantly different from those obtained with the 2 M NaCl procedure or the LIS preparation. It may seem daunting to have three different preparations for a cell structure that has often seemed somewhat ambiguous. Each procedure has important virtues and inevitable defects. Each serves to illuminate different aspects of a biochemically complex structure. In concert, they serve as powerful analytical tools for the study of matrix structure and function.

The LIS prepared matrix (41) is effective principally in displaying DNA attachment sites, at least in *Drosophila* cells. In our hands, the LIS procedure fails to separate chromatin proteins from the matrix. It is likely that the low ionic strength used with the detergent results in adventitious binding of proteins to the matrix. The LIS matrix also has lost all RNP. The preparation is clearly not suitable, at its present stage, for biochemical analysis of proteins or RNA.

The 2 M NaCl procedure (6, 8) releases histones as the first step in separating chromatin from the nucleus. The distended chromatin serves for the analysis of matrix-adjacent DNA sequences. The 2 M NaCl matrix has a very different morphology and probably different biochemical properties. Nevertheless, the 2 M NaCl matrix seems best suited for the study of DNA replication hormone binding sites. The 2 M NaCl matrix also retains hnRNA though not its associated proteins. The RNP-depleted nuclear matrix described here is most like the 2 M NaCl matrix but is not as well suited for examining chromatin loop attachment sites. The RNP-depleted nuclear matrix seems best suited for the study of tissue-specific nuclear composition, structure, and function. It also serves to reveal the role of hnRNP in the nuclear matrix organization.

The nuclear matrix is complex both in composition and morphology in keeping with its known and its postulated functions. The structure carries the DNA replication sites and the attachment points for the chromatin loops. The task of organizing a meter of DNA into the 10-μm-diam mammalian cell nucleus and folding it into compact mitotic chromosomes is formidable. It evidently requires an organizing armature or matrix of considerable structural complexity. A possible clue to the functional significance of the nuclear matrix is afforded by comparing its composition in different cell types. The cell type–specific proteins of the nucleus are largely in the RNP-depleted matrix (22). Matrix composition varies far more than chromatin or cytoplasmic fractions. Such changes indicate the interior matrix may play a significant role in determining chromatin function.

This work was supported by grants from the National Institutes of Health, CA 08416 and CA 37330, and from the National Science Foundation, DCB 8309334.

Received for publication 16 August 1985, and in revised form 29 January 1986.

References

1. Andserson, T. F. 1951. Techniques for the preservation of three dimensional structure in preparing specimens for the electron microscope. *Trans. N.Y. Acad. Sci. Ser. II.* 13:130–134.

2. Barrack, E. R., and D. S. Coffey. 1980. The specific binding of estrogens and androgens to the nuclear matrix of sex hormone responsive tissues. *J. Biol. Chem.* 255:7265–7275.

3. Berezney, R. 1980. Fractionation of the nuclear matrix I. Partial separation into matrix protein fibrils and a residual ribonucleoprotein fraction. *J. Cell Biol.* 85:641–650.

4. Berezney, R. 1984. Organization and functions of the nuclear matrix. *In* Nonhistone Chromosomal Proteins Vol IV: Structural Associations. L. Hnilica, editor. CRC Press, Boca Raton, FL. 119–180.

5. Berezney, R., and L. A. Buchholtz. 1981. Dynamic association of replicating DNA fragments with the nuclear matrix of regenerating liver. *Exp. Cell Res.* 132:1–13.

6. Berezney, R., and D. S. Coffey. 1974. Identification of a nuclear protein matrix. *Biochem. Biophys. Res. Commun.* 60:1410–1417.

7. Berezney, R., and D. S. Coffey. 1975. Nuclear protein matrix: association with newly synthesized DNA. *Science (Wash. DC).* 189:291–292.

8. Berezney, R., and D. S. Coffey. 1977. Nuclear matrix isolation and characterization of a framework structure from rat liver nuclei. *J. Cell Biol.* 73:616–637.

9. Bernhard, W. 1969. A new staining procedure for electron microscopical cytology. *J. Ultrastruct. Res.* 27:250–262.

10. Bernhard, W., and N. Granboulan. 1963. The fine structure of the cancer cell nucleus. *Exp. Cell Res. Suppl.* 9:19–53.

11. Beyer, A. L., M. E. Christensen, B. W. Walker, and W. M. LeStourgeon. 1977. Identification and characterization of the packaging proteins of core 40S hnRNP particles. *Cell.* 11:127–138.

12. Brasch, K. 1982. Fine structure and localization of the nuclear matrix in situ. *Exp. Cell Res.* 140:161–171.

13. Capco, D. G., G. Krochmalnic, and S. Penman. 1984. A new method of preparing embedment-free sections for transmission electron microscopy: applications to the cytoskeletal framework and other three-dimensional networks. *J. Cell Biol.* 98:1878–1885.

14. Capco, D. G., K. M. Wan, and S. Penman. 1982. The nuclear matrix: three-dimensional architecture and protein composition. *Cell.* 29:847–858.

15. Ciejek, E. M., Tsai, M.-J. and B. W. O'Malley. 1983. Actively transcribed genes are associated with the nuclear matrix. *Nature (Lond.).* 306:607–609.

16. Comings, D. E., and T. A. Okada. 1976. Nuclear proteins III: the fibrillar nature of the nuclear matrix. *Exp. Cell Res.* 103:341–360.

17. Diamond, D. A., and E. R. Barrack. 1984. The relationship of androgen receptor levels to androgen responsiveness in the Dunning R3327 rat prostate tumor sublines. *J. Urol.* 132:821–827.

18. Dyson, P. J., P. R. Cook, S. Searle, and J. A. Wyke. 1985. The chromatin structure of Rous Sarcoma provirus is changed by factors that act in trans in cell hybrids. *EMBO (Eur. Mol. Biol. Organ.) J.* 14:413–420.

19. Fakan, S., and W. Bernhard. 1971. Localization of rapidly and slowly labeled nuclear RNA as visualized by high resolution autoradiography. *Exp. Cell Res.* 67:129–141.

20. Fakan, S., E. Puvion, and G. Spohr. 1976. Localization and characterization of newly synthesized nuclear RNA in isolated rat hepatocytes. *Exp. Cell Res.* 99:155–164.

21. Fey, E. G., and S. Penman. 1984. Tumor promoters induce a specific morphological signature in the nuclear matrix-intermediate filament scaffold of Madin-Darby canine kidney (MDCK) cell colonies. *Proc. Natl. Acad. Sci. USA.* 81:4409–4413.

22. Fey, E. G., and S. Penman. 1986. The morphological oncogenic signature: reorganization of epithelial cytoarchitecture and metabolic regulation by tumor promoters and by transformation. Developmental Biology. Vol. 3. The Cell Surface in Development and Cancer. M. Steinberg, editor. In press.

23. Fey, E. G., K. M. Wan, and S. Penman. 1984. Epithelial cytoskeletal framework and nuclear matrix-intermediate filament scaffold: three-dimensional organization and protein composition. *J. Cell Biol.* 98:1973–1984.

24. Fisher, P. A., M. Berrios, and G. Blobel. 1982. Isolation and characterization of a proteinaeous subnuclear fraction composed of nuclear matrix, peripheral lamina and nuclear pore complexes from embryos of *Drosophila melanogaster. J. Cell Biol.* 92:674–686.

25. Franke, W. W., E. Schmid, K. Weber, and M. Osborn. 1979. HeLa cells contain intermediate-sized filaments of the pre-keratin type. *Exp. Cell Res.* 118:95–109.

26. Gallinaro, H., E. Puvion, L. Kister, and M. Jacob. 1983. Nuclear matrix and hnRNP share a common structural constituent with premessenger RNA. *EMBO (Eur. Mol. Biol. Organ.) J.* 2:953–960.

27. Gerace, L., and G. Blobel. 1980. The nuclear envelope lamina is reversibly depolymerized during mitosis. *Cell.* 19:277–287.

28. Gerace, L., A. Blum, and G. Blobel. 1978. Immunocytochemical localization of the major polypeptides of the nuclear pore complex-lamina fraction. Interphase and mitotic distribution. *J. Cell Biol.* 79:546–566.

29. Guatelli, J. C., K. R. Porter, K. L. Anderson, and D. P. Boggs. 1982. Ultrastructure of the cytoplasmic and nuclear matrices of human lymphocytes observed using high voltage electron microscopy of embedment-free sections. *Biol. Cell.* 43:69–80.

30. Hawkes, R., E. Niday, and J. Gordon. 1982. A dot-immunobinding assay for monoclonal and other antibodies. *Anal. Biochem.* 119:142–147.

31. Hentzen, P. C., J. H. Rho, and I. Bekhor. 1984. Nuclear matrix DNA from chicken erythrocytes contains b-globin gene sequences. *Proc. Natl. Acad. Sci. USA.* 81:304–307.

32. Herman, R., L. Weymouth, and S. Penman. 1978. Heterogeneous nuclear RNA-protein fibers in chromatin-depleted nuclei. *J. Cell Biol.* 78:663–674.

33. Jackson, D. A., P. R. Cook, and S. B. Patel. 1984. Attachment of repeated sequences to the nuclear cage. *Nucleic Acids Res.* 12:6709–6726.

34. Jackson, D. A., S. J. McCready, and P. R. Cook. 1981. RNA is synthesized at the nuclear cage. *Nature (Lond.).* 292:552–555.

35. Kish, V. M., and T. Pederson. 1975. Ribonucleoprotein organization of polyadenylate sequences in HeLa cell heterogeneous nuclear RNA. *J. Mol. Biol.* 95:227–238.

36. Laemmli, U. K. 1970. Cleavage of structural proteins during the assembly of the head of bacteriophages T4. *Nature (Lond.).* 227:680–685.

37. Long, B. H., C.-Y. Huang, and A. O. Pogo. 1979. Isolation and characterization of the nuclear matrix in Friend erythroleukemia cells: chromatin and hnRNA interactions with the nuclear matrix. *Cell.* 18:1079–1090.

38. Maundrell, K., E. S. Maxwell, E. Puvion, and K. Scherrer. 1981. The nuclear matrix of duck erythroblasts is associated with globin mRNA coding sequences but not with the major 40S nuclear RNP. *Exp. Cell Res.* 136:435–445.

39. McCready, S. J., J. Godwin, D. W. Mason, I. A. Brazell, and P. R. Cook. 1980. DNA is replicated at the nuclear cage. *J. Cell Sci.* 46:365–386.

40. Miller, T. E., C.-Y. Huang, and A. O. Pogo. 1978. Rat liver nuclear skeleton and ribonucleoprotein complexes containing hnRNA. *J. Cell Biol.* 76:675–691.

41. Mirkovitch, J., M.-E. Mirault, and U. K. Laemmli. 1984. Organization of the higher-order chromatin loop: specific DNA attachment sites on nuclear scaffold. *Cell.* 39:223–232.

42. Monneron, A., and W. Bernhard. 1969. Fine structural organization of the interphase nucleus in some mammalian cells. *J. Ultrastruct. Res.* 27:266–288.

43. Narayan, K. S., W. J. Steele, K. Smetana, and H. Busch. 1967. Ultrastructural aspects of the ribonucleoprotein network in the nuclei of Walker tumor and rat liver. *Exp. Cell Res.* 46:65–77.

44. Nash, R. E., E. Puvion, and W. Bernhard. 1975. Perichromatin fibrils as components of rapidly labeled extranucleolar RNA. *J. Ultrastruct. Res.* 53:395–405.

45. Nelkin, B. D., D. Pardoll, and B. Vogelstein. 1980. Localization of SV-40 genes within supercoiled loop domains. *Nucleic Acids Res.* 8:5623–5633.

46. O'Farrell, P. H. 1975. High-resolution two-dimensional electrophoresis of proteins. *J. Biol. Chem.* 250:4007–4021.

47. Pardoll, D. M., B. Vogelstein, and D. S. Coffey. 1980. A fixed site of DNA replication in eukaryotic cells. *Cell.* 19:527–536.

48. Pederson, T. 1974. Proteins associated with heterogeneous nuclear RNA in eukaryotic cells. *J. Mol. Biol.* 83:163–184.

49. Pederson, T., and N. G. Davis. 1980. Messenger RNA processing and nuclear structure: isolation of nuclear ribonucleoprotein particles containing b-globin messenger RNA precursors. *J. Cell Biol.* 87:47–54.

50. Pullman, J. M., and T. E. Martin. 1983. Reconstitution of nucleoprotein complexes with mammalian heterogeneous nuclear ribonucleoprotein (hnRNP) core proteins. *J. Cell Biol.* 97:99–111.

51. Puvion, E., and W. Bernhard. 1975. Ribonucleoprotein components in liver cell nuclei as visualized by cryo-ultramicrotomy. *J. Cell Biol.* 67:200–214.

52. Robinson, S. I., B. D. Nelkin, and B. Vogelstein. 1982. The ovalbumin gene is associated with the nuclear matrix of chicken oviduct cells. *Cell.* 28:99–106.

53. Ross, D. A., R. W. Yen, and C. B. Chae. 1982. Association of globin ribonucleic acid and its precursors with the chicken erythroblast nuclear matrix. *Biochemistry.* 21:764–771.

54. Samarina, O. P., E. M. Lukanidin, J. Molnar, and G. P. Georgiev. 1968. Structural organization of nuclear complexes containing DNA-like RNA. *J. Mol. Biol.* 33:251–263.

55. Small, D., B. Nelkin, and B. Vogelstein. 1985. The association of transcribed genes with the nuclear matrix of Drosophila cells during heat shock. *Nucleic Acids Res.* 13:2413–2431.

56. Staufenbiel, M., and W. Deppert. 1982. Intermediate filament systems are collapsed onto the nuclear surface after isolation of nuclei from tissue culture cells. *Exp. Cell Res.* 138:207–214.

57. Staufenbiel, M., and W. Deppert. 1984. Preparation of nuclear matrices from cultured cells: subfractionation of nuclei in situ. *J. Cell Biol.* 98:1886–1894.

58. Steele, W. J., and H. Busch. 1966. Studies on the ribonucleic acid components of the nuclear ribonucleoprotein network. *Biochem. Biophys. Acta* 129:54–67.

59. Swift, H. 1963. Cytochemical studies on nuclear fine structure. *Exp. Cell Res. Suppl.* 9:54–67.

60. Towbin, H., T. Staehelin, and J. Gordon. 1979. Electrophoretic transfer of protein from polyacrylamide gels to nitrocellulose sheets. Procedures and some applications. *Proc. Natl. Acad. Sci. USA.* 76:4350–4354.

61. van Eekelen, C. A. G., and W. J. van Venrooij. 1981. HnRNA and its attachment to a nuclear protein matrix. *J. Cell Biol.* 88:554–563.

62. Vogelstein, B., D. M. Pardoll, and D. S. Coffey. 1980. Supercoiled loops and eukaryotic DNA replication. *Cell.* 22:79–85.

63. Wilchek, M., and M. Gorecki. 1969. Affinity chromatography of bovine pancreatic ribonuclease A. *Eur. J. Biochem.* 11:491–494.

64. Wolosewick, J. 1980. The application of polyethylene glycol (PEG) to electron microscopy. *J. Cell Biol.* 86:675–681.